# A SPICE model for a phase-change memory cell based on the analytical conductivity model*

Wei Yiqun(魏益群)[1], Lin Xinnan(林信南)[1,†], Jia Yuchao(贾宇超)[1], Cui Xiaole(崔小乐)[1], He Jin(何进)[1,2], and Zhang Xing(张兴)[1,3]

[1]The Key Laboratory of Integrated Microsystems, Shenzhen Graduate School of Peking University, Shenzhen 518055, China
[2]Peking University Shenzhen SOC Key Laboratory, PKU-HKUST, Shenzhen-Hong Kong Institute, Shenzhen 518055, China
[3]Key Laboratory of Microelectronic Devices and Circuits, Institute of Microelectronics, School of Electronics and Computer Science, Peking University, Beijing 100871, China

**Abstract:** By way of periphery circuit design of the phase-change memory, it is necessary to present an accurate compact model of a phase-change memory cell for the circuit simulation. Compared with the present model, the model presented in this work includes an analytical conductivity model, which is deduced by means of the carrier transport theory instead of the fitting model based on the measurement. In addition, this model includes an analytical temperature model based on the 1D heat-transfer equation and the phase-transition dynamic model based on the JMA equation to simulate the phase-change process. The above models for phase-change memory are integrated by using Verilog-A language, and results show that this model is able to simulate the $I$–$V$ characteristics and the programming characteristics accurately.

**Key words:** phase-change memory; compact model; analytical; conductivity
**DOI:** 10.1088/1674-4926/33/11/114004 **PACC:** 7280; 9160H; 8220W

## 1. Introduction

As the most promising candidate for next generation non-volatile memory, phase-change memory (PCM) has been paid more and more attention, due to its merits of high speed, high density, low power, low cost, long endurance, etc.[1−4]. The programming operation of PCM is based on the quick switch between the crystalline state and the amorphous state in some chalcogonides (like $Ge_2Sb_2Te_5$, namely GST), which is a thermal-driven process. For the design of the periphery circuit, it is necessary to present an accurate SPICE model of a phase-change memory cell (PCM cell) for the purpose of circuit simulation.

In past works, some SPICE models of PCM have been implemented[5−7]. In these models, the resistance of the reset state and the set state are based on a fitting model achieved from the measurement data. The conductivity of the reset or set state are always considered to be constants or the empirical model, which can not reflect the carrier transport characteristics of materials and the device scaling characteristics. Accordingly, an analytical conductivity model including the material transport characteristics is presented. In this work, a PCM cell compact model is proposed, including the analytical conductivity model, the analytical temperature model, and the switch model. The analytical conductivity model calculates the resistance of the PCM cell; the temperature model evaluates the temperature of the programming region; and the phase-change model records the phase fraction. This model provides structural parameters for adjustments and is verified by experimental data and numerical simulations.

## 2. Model description

According to the mechanism of PCM, the reset operation is a phase transition from a crystalline to an amorphous state driven by the fast quenching after melting; the set operation includes two reversible switches. The first is the field-driven ovonic threshold switch (OTS)[8]. Following the OTS, the phase transition from amorphous to crystalline state occurs, called the ovonic memory switch (OMS)[8], driven by Joule heating. Therefore, the model is composed of three parts: the resistance model, the temperature model, and the switch model, as shown in Fig. 1.

### 2.1. Resistance module

The resistance of a PCM cell is the key parameter in pe-

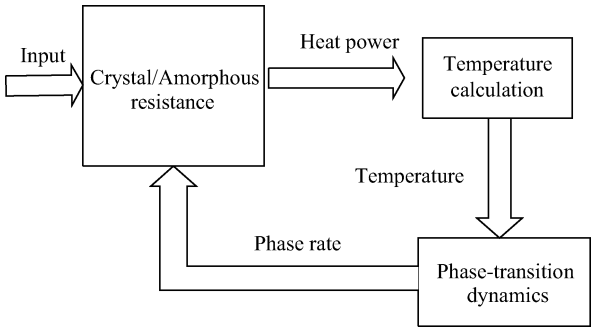


Fig. 1. Scheme of the model.

* Project supported by the National Natural Science Foundation of China (Nos. 61176099, 61006032, 60925015).
† Corresponding author. Email: xnlin@pkusz.edu.cn
Received 17 April 2012, revised manuscript received 8 May 2012

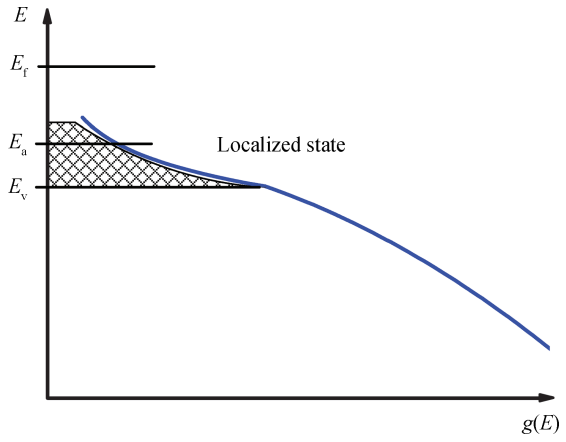


Fig. 2. Band structure model.

riphery circuit design, which determines the details of the circuit design and the performance of the circuit. In our model, an analytical conductivity model is presented, which is based on the carrier transport characteristics of the phase-change material (GST in this work) instead of the fitting model based on the measurement data. According to Anderson's theory[10, 11], in an amorphous semiconductor the long-range disorder of an atomic structure yields the localized state in the conduction band tail and the valence band tail. Amorphous GST is a p-type semiconductor, and the localized state due to lone pairs locates only in the valence band tail[8], so the hole transport characteristics needs to be researched, neglecting the electron transport. The conductivity is determined by:

$$\sigma = qN_{\rm v}\mu. \tag{1}$$

According to the band structure from Ref. [11], the DOS (density of states) function of the band tail satisfies the exponential function of energy, as shown in Fig. 2, so the DOS function can be written by:

$$g(E) = A(E_{\rm a} - E_{\rm v}){\rm e}^{-\frac{E-E_{\rm v}}{E_{\rm a}-E_{\rm v}}}, \tag{2}$$

where $E_{\rm a}$ is the location of $g(E_{\rm v})$ decreasing to $\frac{g(E_{\rm v})}{e}$, as shown in Fig. 2.

The hole density can be calculated by

$$\begin{aligned} p_{\rm a} &= \int_{E_{\rm v}}^{E_{\rm a}} [1 - f(E)]g(E){\rm d}E \\ &= \int_{E_{\rm v}}^{E_{\rm a}} {\rm e}^{-\frac{E_{\rm F}-E}{kT}} \cdot A(E_{\rm a} - E_{\rm v})^{\frac{1}{2}}{\rm e}^{-\frac{E-E_{\rm v}}{E_{\rm a}-E_{\rm v}}}{\rm d}E \\ &\approx \frac{AkT}{e}(E_{\rm a} - E_{\rm v})^{\frac{1}{2}}{\rm e}^{-\frac{E_{\rm a}-E_{\rm F}}{kT}}. \end{aligned} \tag{3}$$

The transport of carrier mobility in a localized state is based on hopping transport mechanism[13], it can be determined by the product of hopping probability $P$ and hopping distance $R$,

$$\mu_{\rm a} = PR = 2\nu_{\rm ph}R{\rm e}^{-\frac{2R}{\alpha}\frac{\Delta W}{kT}}\sinh\frac{qER}{2kT}, \tag{4}$$

where $\nu_{\rm ph}$, $R$, $\Delta W$, $E$ are vibration frequency of phonon, mean hopping distance of hole, barrier height of localized state, and electrical field strength, respectively. The conductivity of amorphous GST can be written by:

$$\begin{aligned} \sigma_{\rm a} = p_{\rm a}q\mu = \frac{p_{\rm a}qRP}{E} &= \sigma_1{\rm e}^{-\frac{E_{\rm a}-E_{\rm v}}{kT}}\frac{\sinh\frac{qER}{2kT}}{\frac{qER}{2kT}} \\ &= \sigma_1{\rm e}^{-\frac{\Delta E_1}{kT}}\frac{\sinh\frac{qER}{2kT}}{\frac{qER}{2kT}}, \end{aligned} \tag{5}$$

where $\sigma_1$ is the fitting parameter, defined by $\nu_{\rm ph}$, $\Delta W$, $\alpha$. The values of parameters are listed in Table 1.

The conductivity of crystal GST can be calculated by using traditional semiconductor theory and the $I$–$V$ characteristics of amorphous and crystal GST. As for the detailed device, as shown in Fig. 3, with the width of heater $D_{\rm h} = 70$ nm, the whole resistance can be calculated by the conductivities of amorphous and crystal GST, the $I$–$V$ curve is shown in Fig. 4. From Fig. 4, it is indicated that the $I$–$V$ characteristic exhibits a linear relation under lower bias and the exponential relation under higher bias, which satisfies the hopping transport mechanism.

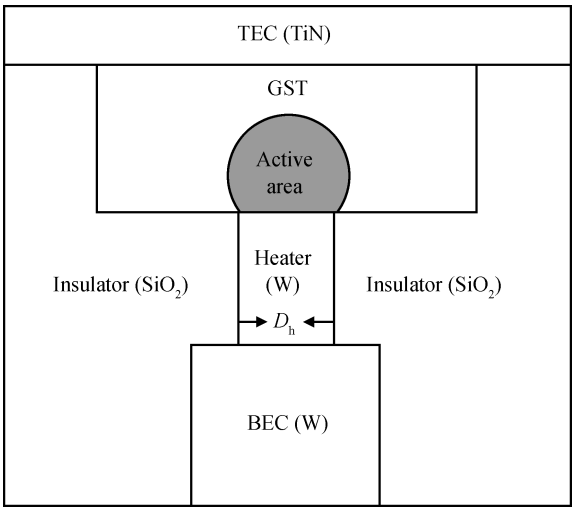


Fig. 3. Structure of a PCM cell.

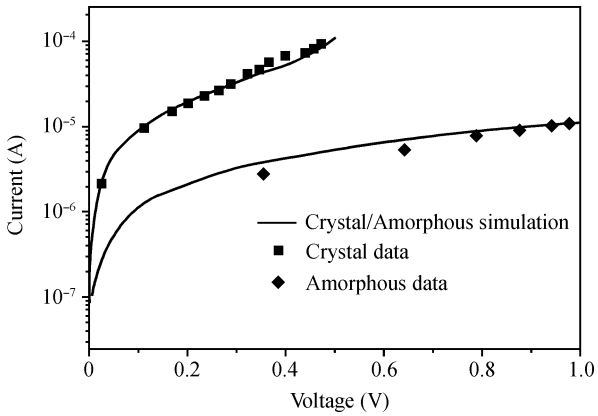


Fig. 4. $I$–$V$ curves for the crystal state and the amorphous state.

Table 1. Parameter list.

| Parameter | Value |
|---|---|
| $A$ (Fitting parameter of DOS function) | $2 \times 10^{16}$ cm$^{-3}$ |
| $\sigma_1$ (Fitting electrical conductivity) | $1.667 \times 10^5$ $(\Omega\cdot m)^{-1}$ |
| $\Delta E_1$ (Energy gap between $E_a$ and $E_V$) | 0.45 eV[14] |
| $R$ (Mean hopping distance of carrier) | $1.5 \times 10^{-5}$ cm |
| $K$ (Thermal conductivity) | 0.005 W/(cm·K)[15] |
| $c$ (Heat capacity) | 1.285 J/(cm$^3$·K)[15] |
| $t_0$ (Time constant of JMAK equation) | $2 \times 10^{-36}$ s[16] |
| $E_a$ (Activation energy of nucleation) | 3.7 eV[16] |

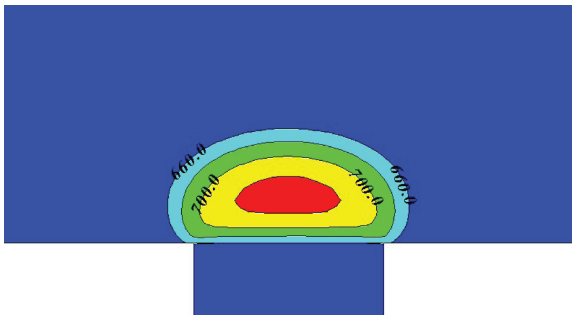

Fig. 5. Temperature distribution of the numerical simulation.

### 2.2. Temperature model

According to the numerical simulation, the temperature distribution is not uniform in the device, as shown in Fig. 5, and it is very difficult to model the temperature distribution. However, in the programming area, we can see that the relative error for maximum and minimum temperature is about 7%, and the programming area can be deemed as an isothermal area. Based on the above assumption, an analytical temperature model is proposed.

The temperature can be determined by the difference of power generation and power dissipation. The generation power is the product of current and voltage, with an effective coefficient $\beta$, determined by:

$$W_g = \beta I V. \tag{6}$$

Following the power generation, the power dissipation happens simultaneously, and it can be determined by a 1-D heat transfer equation:

$$W_d = \frac{\partial Q}{\partial T} = \frac{\kappa \Delta T}{R_t} S_t, \tag{7}$$

where $\kappa$, $R_t$, $S_t$, are the thermal conductivity, the average distance from heating point to a room-temperature environment, which is linear to the temperature, and the thermal cross-section area, respectively. The temperature increment $\Delta T$ from the environment is determined by the above differential equation:

$$\Delta T = \int_{t_0}^{t_1} \frac{W_g - W_d}{C V_0} \mathrm{d}t = \frac{W_g R_t}{\kappa S_t} \left[1 - \exp\left(-\frac{\kappa S_t}{R_t V_0 C} t\right)\right], \tag{8}$$

where $C$ is the heat capacity of GST material and $V_0$ is the volume of the effective heating region.

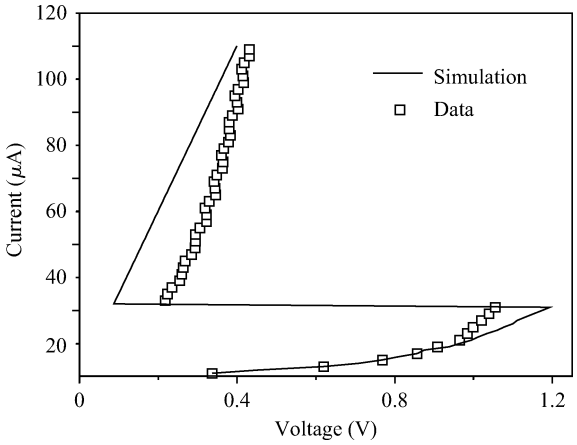


Fig. 6. $I$–$V$ curves.

### 2.3. Switch model

OTS and OMS are included in our model. As for OTS, a model based on critical electrical field strength[8] is accepted. When the electrical field strength in the device reaches a critical value $E_c$, the OTS happens, and the value of $E_c$ is equal to $10^7$ V/cm for fitting the measured data.

The OMS process includes two transitions: one is the reset process; the other is the set process. The former is modeled by a temperature-conditioned model. If the temperature of the PCM cell is higher than the melting point, the resistance of the active area is set to the amorphous resistance value. The latter is a more complex process, which is the nucleation process with proper temperature. In this model, the JMA equation is used to calculate the fraction of crystalline composition in the active region by temperature and time[6]. The crystalline fraction $C_c$ is given by Eq. (9).

$$C_c = 1 - \exp\left[-\frac{t}{t_0} \exp\left(-\frac{E_a}{kT}\right)\right], \tag{9}$$

where $E_a$ is the activation energy, and $t_0$ is the time constant.

The crystallization model decides the fraction of the crystalline and amorphous region, and feeds it back to the resistance model, and the whole resistance can be modeled by a linear relation,

$$R_{GST} = R_{npc} + R_{ac} C_c + R_{aa}(1 - C_c), \tag{10}$$

where $R_{GST}$, $R_{npc}$, $R_{ac}$, $R_{aa}$ are resistance of the GST region, the non-phase-change region, the crystal, and the amorphous parts in the active area, respectively, and $C_c$ is the nucleation rate, which is to be modeled in the switch model.

The parameters in this model are listed in Table 1.

## 3. Results and discussion

The DC analysis gives out the $I$–$V$ characteristic of this model shown in Fig. 6. From this curve, it is shown that the threshold voltage is about 1.2 V, and the simulation fits the measurement data well in the sub-threshold area. In the area near the threshold area, the larger error derives from the influence of temperature. Figure 7 shows the transient current and temperature curves. The initial state is the reset state, and the first pulse is the set current pulse with an amplitude of

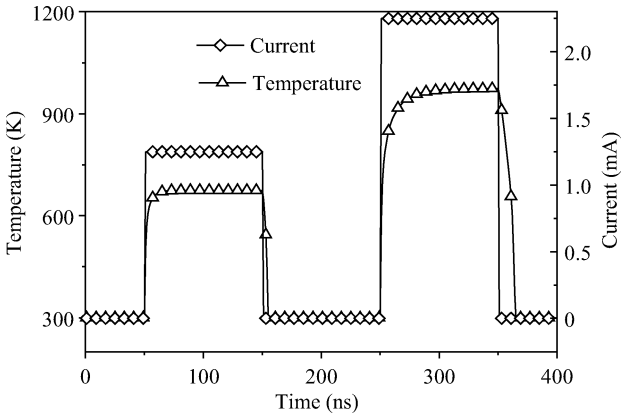


Fig. 7. Temperature curve with different programming pulses.

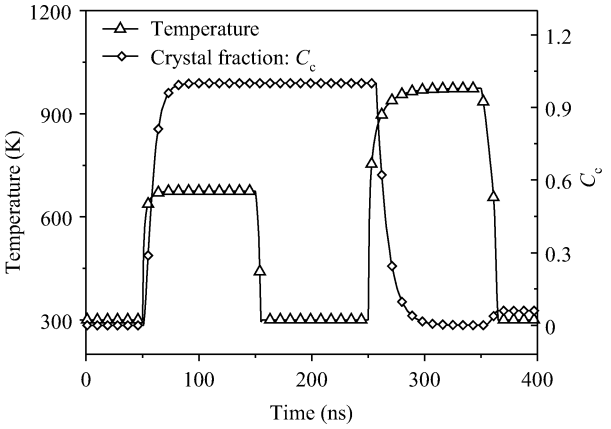


Fig. 8. Phase distribution curve with different temperatures.

1.25 mA, followed by the reset current pulse with an amplitude of 2.25 mA. During the set pulse, the temperature reaches about 700 K between $T_g$ (glass temperature) and $T_m$ (molten temperature), the nucleation fraction $C_c$ reaches about 1, as shown in Fig. 8. The set operation is accomplished. During the reset pulse, the temperature increases to about 1000 K, higher than $T_m$, and the active area melt to liquid state. After the reset pulse is removed, the temperature falls to ambient temperature sharply, and the active area quenches to an amorphous state. The nucleation fraction decreases to about 0, as shown in Fig. 8. The reset operation is accomplished. Figure 9 shows the $I$–$R$ curve, which indicates the programming window. It is shown that the simulation results and the measurement data fit well.

## 4. Conclusion

In summary, this work presents a compact model for a PCM cell, which is achieved by an analytical resistance model based on the transport theory. Compared with the existing model, the set and reset resistances can be calculated according to the analytical physical-based model, whereas the present models are mostly based on the measurement data to obtain the resistance value. Meanwhile accurate DC and transient simulations can be achieved using this model. These model characteristics will help circuit designers predict the performance of a circuit and optimize the circuit design.

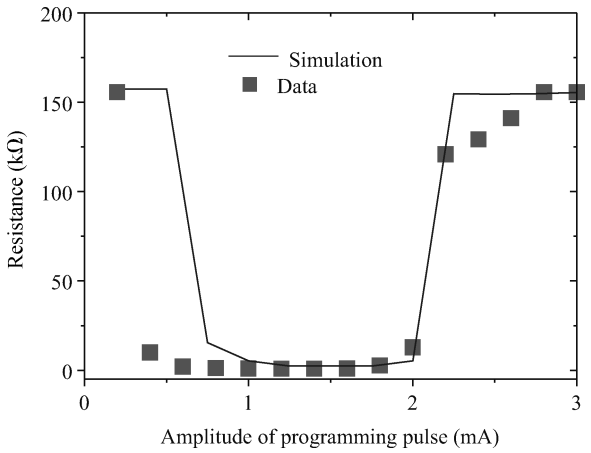


Fig. 9. $I$–$R$ curves.

## Acknowledgement

We would like to thank Mr. Jin Rong for the fruitful discussions.

## References

[1] Lai S. Current status of the phase change memory and its future. IEEE International Electron Devices Meeting, Technical Digest, 2003: 255

[2] Lacaita A L, Ielmini D, Mantegazza D. Status and challenges of phase change memory modeling. Solid-State Electron, 2008, 52: 1443

[3] Xu Cheng, Liu Bo, Chen Yifeng. Switching characteristics of phase change memory cell integrated with metal–oxide–semiconductor field effect transistor. Chin Phys Lett, 2008, 25(5): 1848

[4] Feng Gaoming, Liu Bo, Wu Liangcai, et al. Properties of W submicrotube heater electrode used for phase change memory. Journal of Semiconductors, 2007, 28(7): 1134

[5] Liao Y B, Chen Y K, Chiang M H. An analytical compact PCM model accounting for partial crystallization. Proceedings IEEE International Conference on Electron Devices and Solid-State Circuits, 2007, 1/2: 625

[6] Kwong K C, Li L, He J, et al. Verilog—a model for phase change memory simulation. 9th International Conference on Solid-State and Integrated-Circuit Technology, 2008: 4

[7] Wei X Q, Shi L P, Zhao R, et al. Universal HSPICE model for chalcogenide based phase change memory elements. Proceedings Non-Volatile Memory Technology Symposium, 2004: 88

[8] Li Xi, Song Zhitang, Cai Daolin, et al. An SPICE model for phase-change memory simulations. Journal of Semiconductors, 2011, 32(9): 094011

[9] Pirovano A, Lacaita A L, Benvenuti A, et al. Electronic switching in phase-change memories. IEEE Trans Electron Devices, 2004, 51: 452

[10] Anderson P. Absence of diffusion in certain random lattice. Phys Rev, 1958, 109(5): 1492

[11] Liu Enke, Zhu Bingsheng, Luo Jinsheng. Semiconductor physics. Beijing: National Defense Industry Press, 2003: 354 (in Chinese)

[12] Baranovski S. Charge transport in disordered solids with appli-

cations in electronics. Wiley, 2006: 63
[13] Lelmini D, Zhang Y. Analytical model for subthreshold conduction and threshold switching in chalcogenide-based memory devices. J Appl Phys, 2007, 102: 054517
[14] Kato T, Tanaka K. Electronic properties of amorphous and crystalline $Ge_2Sb_2Te_5$ films. Jpn J Appl Phys, 2005, 44(10): 7340
[15] Peng C, Cheng L, Mansuripur M. Experimental and theoretical investigations of laser-induced crystallization and amorphization in phase-change optical recording media. J Appl Phys, 1997, 82(9): 4183
[16] Technology report of Ovonyx. Http://ovonyx.com/technology/technology.pdf